

Effect on heat transfer for laminar flow over Backward Facing Step with square cylinder placed inside using Higher Order Compact Scheme

Karumanchi Viswanatha Sarma^{1,*}, N Sekarapandian¹, S Vengadesan¹,
Y V S S Sanyasiraju²

¹Dept. of Applied Mechanics, IIT Madras, Chennai-600 036

²Dept. of Mathematics, IIT Madras, Chennai-600 036

Abstract

The purpose of this paper is to study the influence of an adiabatic square cylinder on the heat transfer enhancement in the 2D laminar flow over the Backward Facing Step (BFS). This work also studies the effect of streamwise position of the square cylinder on heat transfer enhancement. The governing equations, for the 2D laminar flow over BFS with a square cylinder placed inside, are solved on non-uniform Cartesian grid using projection method. The individual differential terms of the N -S equations are discretized using a Higher Order Compact Scheme (HOCS). The numerical code is first validated with the results available in the literature. The main advantage of HOCS is to obtain higher order approximations to the derivatives accurately without the necessity of higher number of nodes. Thus reducing the computational cost. It is observed from the numerical experiment that placing the cylinder affects the fluid flow and heat transfer and for $X_C=1.4$, $Y_C = 1.0$ and $Re= 200$, there is a maximum heat transfer enhancement of 193.93%. The results of these numerical experiments are useful in studying the heat transfer enhancement and its dependence on the bluff body and flow characteristics. This work has its applications in engineering problems where the heat transfer in a laminar flow regime can be enhanced using a bluff body. The current work also demonstrates the dependence of horizontal position of cylinder on heat transfer augmentation.

Keywords: Backward Facing Step, Square cylinder, Heat transfer enhancement, Higher Order Compact Scheme, Location of the cylinder;

I. Introduction

The phenomenon of flow separation and reattachment, in fluid dynamics exert an important influence on heat transfer rates and a study of the same has wide range of applications such as the design of aircraft wings, turbines, diffusers, buildings etc.. There is a vast literature dedicated to the study of this topic [1][2][3][4][5][6]. The focus is often to achieve the enhanced heat transfer in laminar regimes. Heat transfer enhancement in laminar flows is often achieved artificially by modifying the flow structure either actively by blowing, sucking, pulsating etc[7][8][9][10][11][12] or passively by placing an obstacle in the path of flow [13][14][15][16].

Only few reports appeared on heat transfer enhancement of BFS flows with an obstacle in the path, placed near the step. The heat transfer enhancement by placing an adiabatic circular obstacle was studied in [17] and [18]. The effect of adiabatic square obstacle on heat transfer enhancement is investigated in [19] and [20]. They performed many numerical experiments by varying the Reynolds number and vertical location of the cylinder. In the present study, an attempt has been made to investigate the heat transfer in a laminar flow over BFS with square obstacle placed in the path. The study includes the effect of various parameters such as Reynolds number, step height, dimensions, location of the obstacle i.e both cross-stream and stream-wise position on the flow and hence on the heat transfer. This particular work further demonstrates the capability of the higher order compact scheme based incompressible flow solver for staggered uniform grid developed in [21] to handle the non-uniform grids. The related non-uniform grid coefficients of the compact schemes used in this work are reported in [22]. To the best knowledge of the authors, effect of horizontal position of square cylinder on heat transfer has not been studied and hence an attempt has been made to study the effect of horizontal position on heat transfer.

II. Problem Description

Schematic of the physical problem along with the boundary conditions are shown in Fig. 1. A channel with backward facing step is considered. Since the effect of entrance length on the reattachment was reported to be very less [17][20], the same is ignored in the present study. The step height 'S' is taken as the non-dimensional length parameter and a channel length of 40S is considered to ensure that the re-circulation length is independent of the physical domain. Channel height of 2S is considered for all the numerical simulations. A square obstacle of size 0.4S is placed behind the backward facing step at three different stream-wise positions viz. $X_C = 0.6S, 1.0S$ and $1.4S$, and three cross-stream positions $Y_C = 0.5S, 1.0S$ and $1.5S$. The flow is assumed to be two-dimensional, incompressible and laminar. No-slip boundary condition is enforced on all the solid surfaces. A parabolic velocity profile and a uniform temperature are fixed in all the computations. The bottom wall is maintained at a non-dimensional temperature of unity and all other solid surfaces are considered as adiabatic. Working fluid is taken as the air with Prandtl number of 0.71. The effect of temperature on the fluid properties like viscosity, density, thermal conductivity etc., is not included in the study.

III. Numerical Scheme

The dimensionless parameters are defined as

$$(U, V) = \frac{(u, v)}{u_0}(X, Y) = \frac{(x, y)}{S},$$

$$\tau = \frac{u_0}{S} t, P = \frac{p}{\rho u_0^2}, \theta = \frac{T - T_1}{T_w - T_1} \quad (1)$$

Governing equations for incompressible, laminar, two-dimensional unsteady case are

$$\vec{U}_t + \nabla P = -\vec{U} \cdot (\nabla \vec{U}) + \frac{1}{Re} \nabla^2 \vec{U}$$

$$\nabla \cdot \vec{U} = 0 \quad (2)$$

$$\theta_t = -\vec{U} \cdot (\nabla \theta) + \frac{1}{RePr} \nabla^2 \theta$$

The boundary conditions for the problem are given as:

- $U = 6(2 - Y)(Y - 1), V = 0$ and $\theta = 0$ at the inlet.
- $\theta = 1$ on the bottom wall, and $\frac{\partial \theta}{\partial n} = 0$ on all the other solid surfaces (adiabatic condition).
- No-slip boundary condition for the velocity i.e. $U = V = 0$ on all the solid surfaces.
- At the outlet $\frac{\partial U}{\partial X} = \frac{\partial V}{\partial X} = 0$

Equation (2) refers to the governing equations for the incompressible fluid flow along with forced convection heat transfer. The numerical algorithm to solve (2) using a fractional step method approach [23] is reported in [21]. The unique feature of the solver used in this work is the discretization of the spatial derivatives using compact schemes derived over non-uniform staggered Cartesian grids. Specifically, the developed schemes can fetch a maximum of third and fourth order spatial accuracy for second and first derivatives, respectively. The complete details on the numerical scheme used in this work are reported in [22].

Solving the (2) along with the above mentioned boundary conditions will yield the values of $U(X, Y), V(X, Y), P(X, Y)$ and $\theta(X, Y)$. From these values streamtraces, local Nusselt number etc. are calculated in the postprocessing.

- The local Nusselt number along the bottom (hot) wall is of main interest and it is defined as:

$$Nu(X) = -\left(\frac{\partial T}{\partial Y}\right) = \frac{hS}{k} \quad (3)$$

- The time averaged Nusselt number over duration time τ is defined as :

$$Nu = \frac{1}{\tau} \int_0^\tau Nu_i dt \quad (4)$$

Where, Nu_i is the instantaneous Nusselt number.

- The space averaged Nusselt number along the bottom wall of length L is defined as :

$$Nu_{Avg} = \frac{1}{L} \int_0^L Nu. dx \quad (5)$$

The time averaged velocity, pressure and temperature are calculated in a similar fashion as given in (4).

The validation studies are carried out initially for no-cylinder case. Four non-uniform structured Cartesian grids, two each for fluid flow validation and thermal validations are considered. Details of the grids are given in the Table 1. Results for the fluid flow validation carried out at $Re=800$ and thermal validation carried out at $Re=100$, are given in the Fig.2. The results are very close and thus confirming the numerical strategies.

Table 1. Grid details for validation

GRID SIZE	X-direction			Y-direction (uniform)
	dx (max)	dx (min)	AR	dy
Fluid flow validation				
277 × 26	0.1993	0.04	4.9825	0.04
737 × 101	0.1998	0.01	19.98	0.01
Thermal Validation				
548 × 51	0.1993	0.04	17.8795	0.04
947 × 101	0.1992	0.02	15.3598	0.02

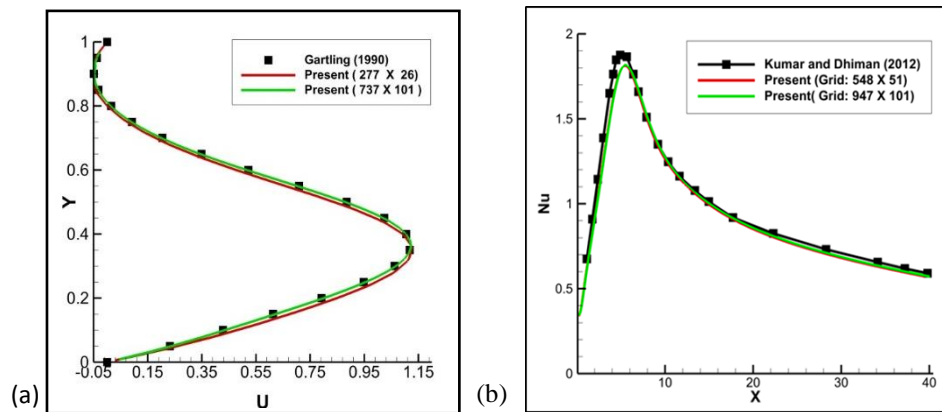


Fig 2. Validation results for (a) Variation of velocity and (b) Nusselt number distribution

IV. Numerical Simulations

The numerical simulations are performed to study the fluid flow and heat transfer for the BFS with square cylinder placed inside. From the previous works [17][18][19] and [20] it is noticed that the flow and heat transfer characteristics depend on various parameters like Reynolds number Re , the Prandtl number Pr , the dimensionless height of the backward facing step S , the dimensionless length of the square d , the stream-wise dimensionless distance between the backward facing step and the center of square cylinder, the cross-stream dimensionless distance between hot bottom face and center of square cylinder, the dimensionless length of the channel L and the expansion ratio (ER) of the geometry.

Though the numerical experiments can be performed for various combinations of these parameters, in the present work, simulations are carried out only on the following selective critical combinations and the results are reported:

1. Reynolds number range $50 \leq Re \leq 200$ in the steps of 50
2. Three different stream-wise positions i.e 0.6, 1.0 and 1.4
3. Three cross-stream positions varied from 0.5 to 1.5 in the steps of 0.5.

A channel of expansion ratio 2 and length $40S$ is considered for all the numerical computations. The focus of the work is to study the influence of the Reynolds number and the position of the obstacle on heat transfer. Hence, for all the numerical calculations the step height $S=1$ is fixed.

Grid independence study is performed for the given physical problem for the case of streamwise position of 0.6, cross-stream position of 1.5 and Re of 200, on two different non-uniform grids. Results of the grid independence study are reported in the Fig.3. The variation between the results of two grids are found to be within 2% and thus negligible.

A structured non-uniform grid of size 538×101 and aspect ratio 25 is used. The values obtained from numerical experiment; averaged over 210 and 190 non-dimensional time are found to be in a good agreement with each other. Hence, numerical values that are averaged for 190 non-dimensional time are reported in the work.

V. Results and Discussions

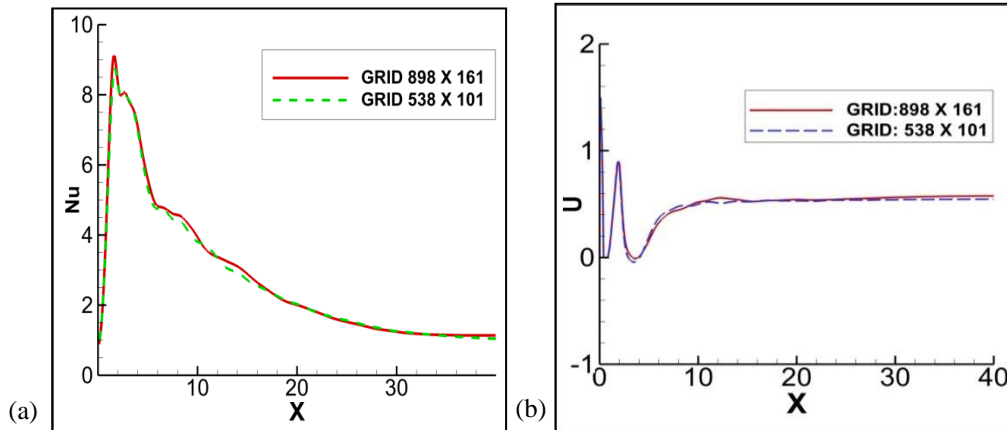


Fig 3 Grid Independent study (a) Mean Nusselt number distribution (b) Mean wake centerline velocity distribution.

a. Fluid Flow Characteristics

In this section, streamline plots are discussed. Figure 4 shows the mean streamline plot of BFS with square cylinder placed inside. All the cases are compared against the no-square cylinder condition. For no obstacle case, which is given at the top for each Re, the recirculation zone adjacent to the step, increases with Reynolds number as shown in the figure. At $Re=200$, a small recirculation region on the top wall can be seen.

The cylinder at $Y_C = 0.5$ has no effect on the recirculation length, when compared to its unobstructed counterpart. The position of the cylinder below the step does not seriously obstruct the flow and thus the flow structure does not alter much from unobstructed case. Also the dividing shear layer between recirculation zone and the flow is not noticed to be affected significantly. The stream-wise position has no effect on the recirculation length, except for dividing the recirculating region into two regions. One recirculating region is observed on the top-left corner of the cylinder and another region along the downstream of the backward facing step. With the ascending stream-wise position, the top-left corner eddy is found to increase in size for any given Reynolds number; this can be due to the space between the cylinder and the step and the fluid flow through this gap. For $Y_C = 1.0$, the top half of the cylinder is above the step and the bottom half is below the step. This has substantial effect on the flow as shown in the figure. Some part of the fluid squeezes into the region underneath the cylinder, through the gap between cylinder and the step. It then re-attaches on the bottom wall, separates from it and entrains into the wake region forming a secondary recirculation bubble on the bottom wall. At $Re > 100$, the formation of recirculation bubbles adjacent to the step is observed. For $Y_C = 1.0$, these recirculation bubbles coalesce into a single large bubble. Size of this bubble does not alter much after $Re=100$ and thus remains constant. Contrary to this, the secondary recirculation zone on the bottom wall breaks up into two zones for stream-wise positions of 1.0 and 1.4 and at $Re=200$. The small recirculation bubble near the cylinder, for $Re > 100$, is seen to grow with increasing stream-wise position.

For $Y_C = 1.5$, the square cylinder is completely above the step and hence more fluid can pass through the gap between the cylinder and step. A primary recirculation zone of almost constant size is also observed near the step. When the Reynolds number is increased, two vortices behind the cylinder, directing downwards are noticed. This can be due to the downward motion of the fluid. At $Re=50$, a secondary recirculation zone is observed on the top wall for $X_C = 1.0$ and $X_C = 1.4$. For $X_C = 0.6$ and $Re=150$, recirculation region with two cores is noticed on the top wall of the channel. The size of this region is seen to decrease with ascending stream-wise position. Moreover, the top channel wall recirculation zone in the case of $Re=200$ increased in length with ascending stream-wise position.

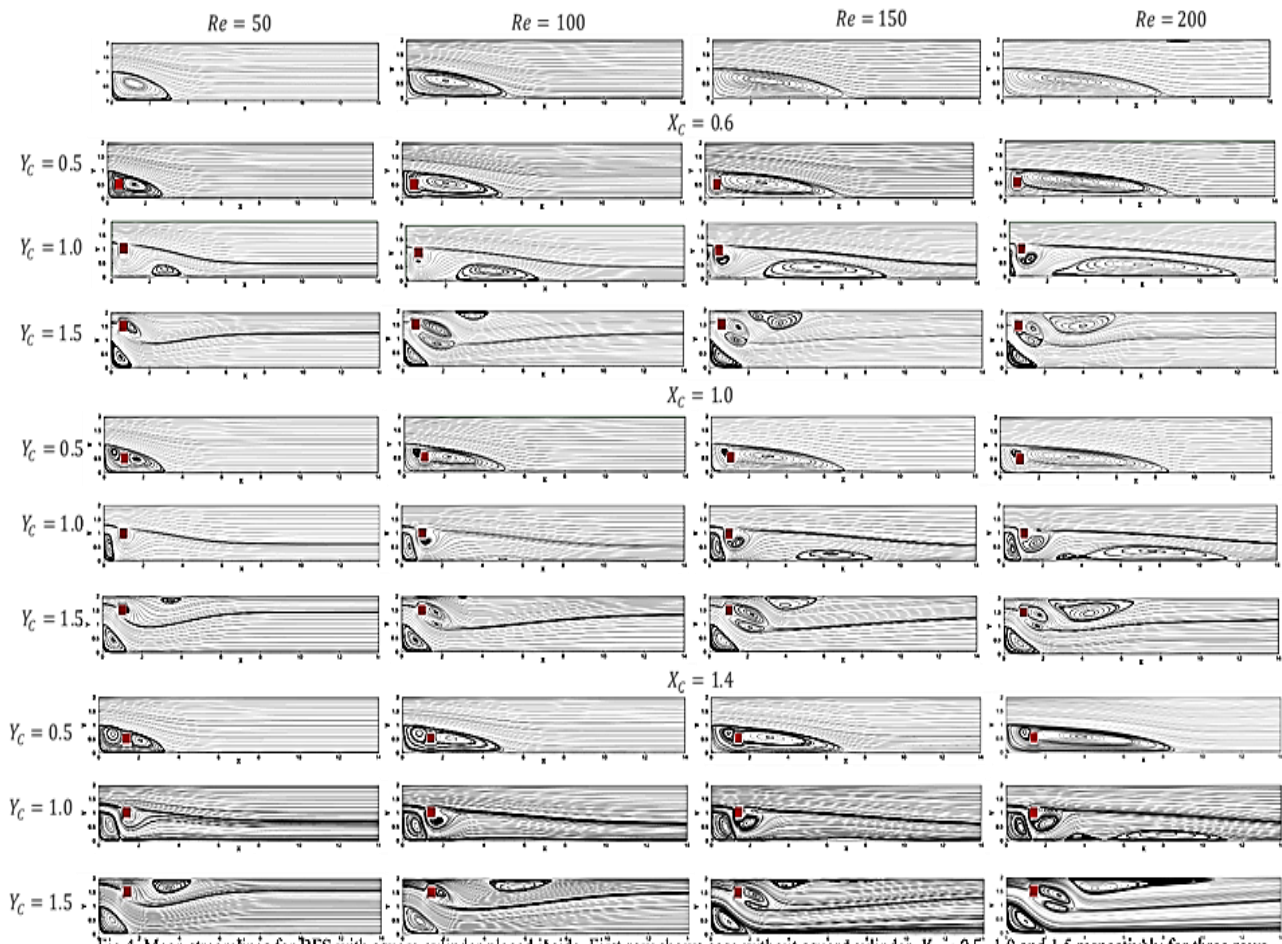


Fig 4. Mean streamlines for BFS with square cylinder placed inside. First row shows case without square cylinder. $Y_C = 0.5, 1.0$ and 1.5 respectively for three rows of each X_C .

b. Heat Transfer Characteristics

i. Local Nusselt Number

Plots for the mean Nusselt number distribution along the bottom wall are shown in Fig. 5. For unobstructed case, the maximum value of the Nusselt number is observed to increase with the increasing Reynolds number. The maximum Nusselt number is appeared to shift towards the step with the increasing Reynolds number. Larger the recirculation zone, better the mixing and hence, better convective flow is observed in the region reflecting the rise in the maximum Nusselt number values.

For $Y_C = 0.5$ there is no variation in the peak value of the Nusselt number compared to the unobstructed case as shown in Fig. 5. In both upstream and downstream directions multiple peaks are noticed for this position. In the case of $X_C = 1.0$, distinct peaks are observed which are increasing in their value with Reynolds number, when compared to those observed for $X_C = 0.6$. For $Y_C = 1.0$ there is a remarkable increase in the maximum Nusselt number value and it is located near the square cylinder. Only a single peak is observed for lower Reynolds numbers at $Y_C = 1.5$ and $X_C = 0.6$. But with $Re > 100$, the highest Nusselt number value is followed by smaller peaks. These may be caused by the presence of vortices behind the cylinder and the secondary recirculation region on the top wall. The maximum Nusselt number in the plot is less compared to that of $Y_C = 1.0$. At all the streamwise locations minor peaks in the Nusselt number plots are absent for cross-stream positions higher than 0.5. For $X_C = 1.4$ and $Y_C = 1.0$ at $Re=200$, maximum value of the Nusselt number is highest among all the cases considered as seen in Fig. 5. The stream-wise position is found to affect the maximum value of the Nusselt number which may be due to the variations in the recirculation zones in the downstream direction.

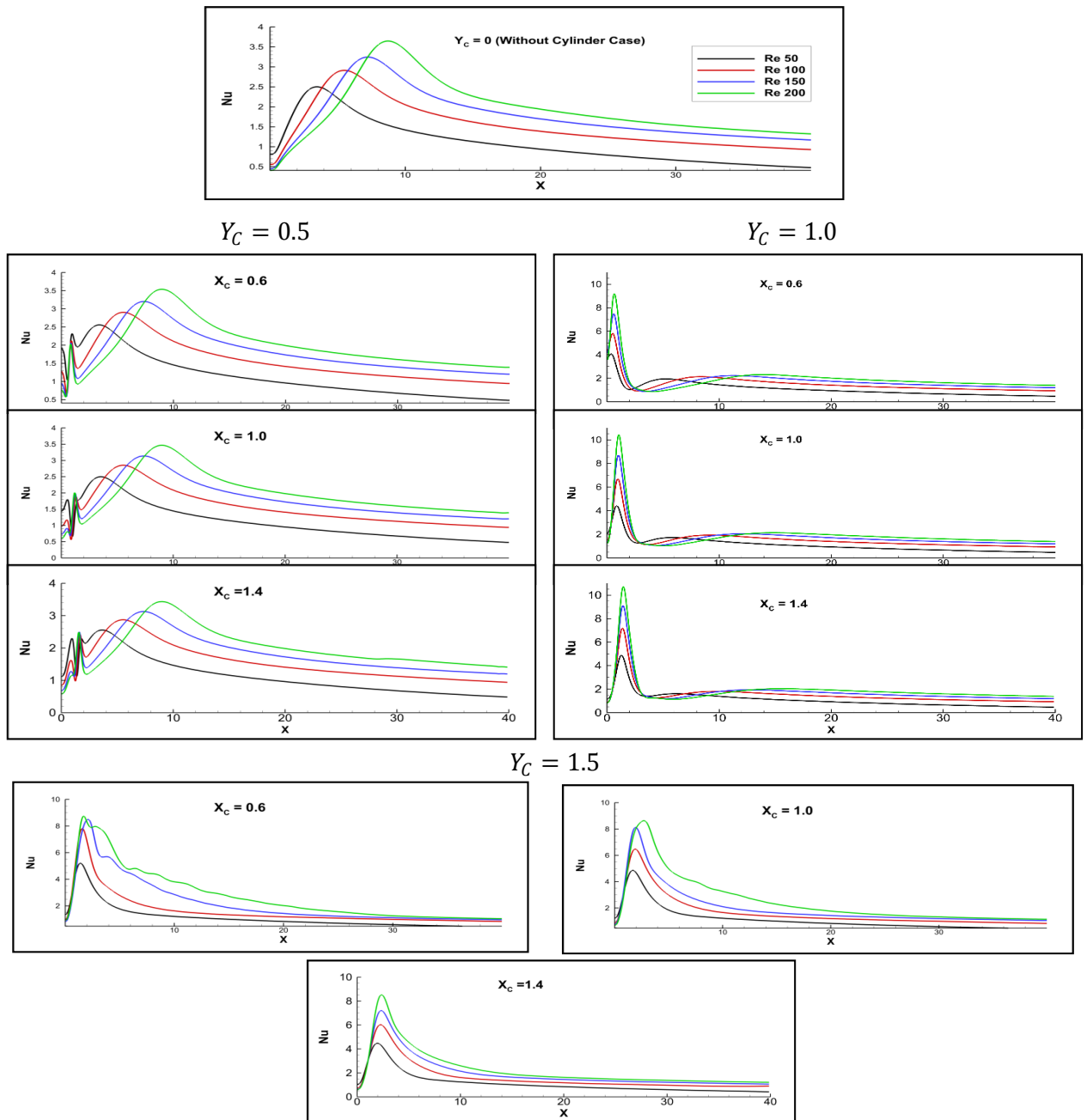


Fig 5. Mean local Nusselt number plots along bottom channel wall of BFS

ii. Average and maximum Nusselt numbers

Plots for average Nusselt number are presented in Fig. 6. The average Nusselt number along the bottom wall of the channel is computed by space averaging the time averaged Nusselt number obtained from the numerical simulation. The average Nusselt number value is seen to increase with increasing Reynolds number. The slope of the curve for a given stream-wise position, is found to be highest for $Y_C = 1.5$. The variation of Nu_{Avg} values with Reynolds number is exhibiting similar trend for all the stream-wise positions. The values of Nu_{Avg} at a given elevation and Reynolds number are remaining nearly same for all the stream-wise positions.

To compare the effect of the square cylinder in the backward facing step with that of unobstructed case, $Nu_{Max} / Nu_{Max,Unobstructed}$ versus Reynolds number is plotted for various cross stream positions in the Fig. 7. The figure shows the monotonic increase in the ratio $Nu_{Max} / Nu_{Max,Unobstructed}$, with the Reynolds number for all stream-wise positions of the cylinder. The plots for $Y_C > 0.5$ tend to intersect as seen in the figure. The intersection point tends to move towards the lower Reynolds numbers and finally is absent for $X_C = 1.4$. At $X_C = 1.4, Y_C = 1.0$ and for $Re = 200$, $Nu_{Max} / Nu_{Max,Unobstructed}$ is 2.93 indicating an increase of about 193% in the peak Nusselt number which

is highest of all the cases. This shows the significant effect of streamwise position on the heat transfer enhancement when compared to the previous works [19][20].

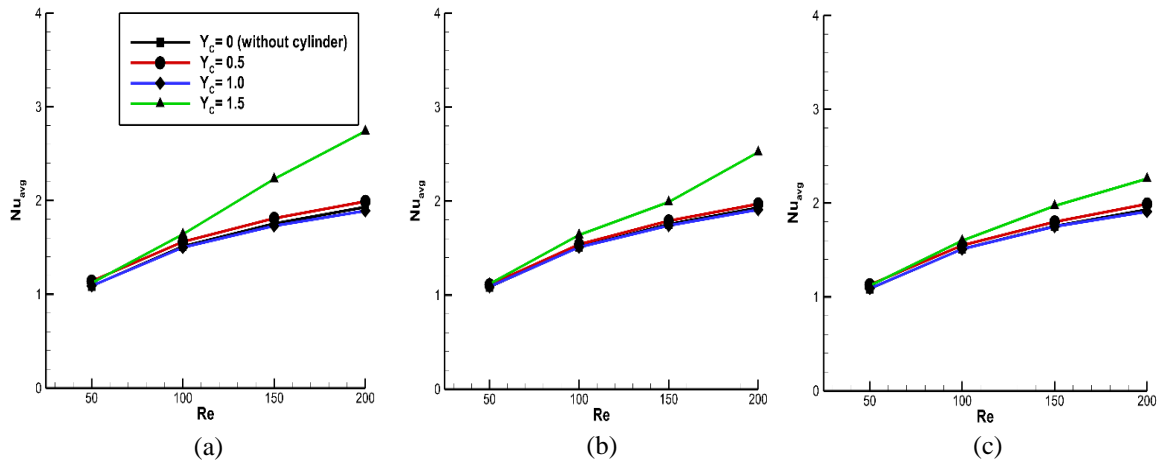


Fig 6. Variation of Nu_{Avg} versus Reynolds number for (a) $X_C = 0.6$ (b) $X_C = 1.0$ and (c) $X_C = 1.4$ for the given cross-stream position and Reynolds number.

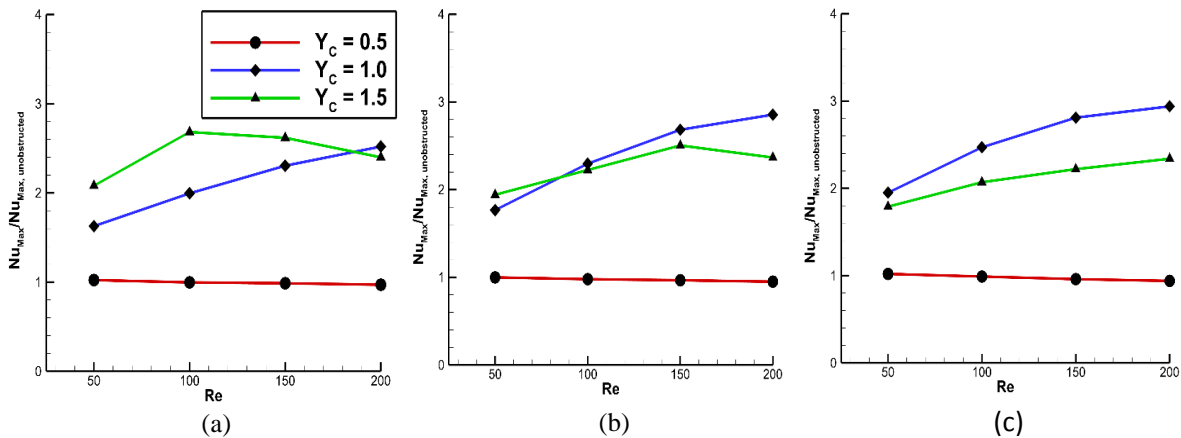


Fig 7. Variation of $Nu_{Max}/Nu_{Max,Unobstructed}$ versus Reynolds number for (a) $X_C = 0.6$ (b) $X_C = 1.0$ and (c) $X_C = 1.4$ for the given cross-stream position and Reynolds number.

VI. Conclusions

In the present work, fluid flow and heat transfer properties of downstream of the backward facing step with square cylinder placed as an obstacle are studied. The numerical simulations are carried out at $Re=50, 100, 150, 200$ and $Pr=0.71$. The heat transfer enhancements for the same are studied by choosing an adiabatic square cylinder in three cross-stream locations of 0.5, 1.0 and 1.5, and three stream-wise locations of 0.6, 1.0 and 1.4. Variations of mean streamline and local Nusselt number distributions with different parameters are studied. Location of the cylinder is found to affect the recirculation region and in turn the heat transfer along the bottom wall. For a given set of conditions, it is observed that the placement of square cylinder is effective in augmenting the heat transfer. The results show that the heat transfer reaches its maximum with an enhancement of about 193% compared to an unobstructed case, for stream-wise position of 1.4, cross-stream position of 1.0 and Reynolds number of 200. This work highlights the dependence of heat-transfer enhancement on stream-wise position in addition to the cross-stream position.

References

- [1] Armaly, B. F., Durst, F., Pereira, J. C. F., and Schönung, B. (1983). Experimental and theoretical investigation of backward-facing step flow. *Journal of Fluid Mechanics*, 127, 473-496.
- [2] Gartling, D. K. (1990). A test problem for outflow boundary conditions—flow over a backward-facing step. *International Journal for Numerical Methods in Fluids*, 11(7), 953-967.
- [3] Biswas, G., Breuer, M., and Durst, F. (2004). Backward-facing step flows for various expansion ratios at low and moderate Reynolds numbers. *ASME Trans. Journal of Fluids Engineering*, 126(3), 362-374.
- [4] Aung, W. (1983). An experimental study of laminar heat transfer downstream of backsteps. *Journal of Heat Transfer*, 105(4), 823-829.
- [5] Kondoh, T., Nagano, Y., and Tsuji, T. (1993). Computational study of laminar heat transfer downstream of a backward-facing step. *International Journal of heat and mass transfer*, 36(3), 577-591.
- [6] Turki, S., Abbassi, H., and Nasrallah, S. B. (2003). Two-dimensional laminar fluid flow and heat transfer in a channel with a built-in heated square cylinder. *International Journal of Thermal Sciences*, 42(12), 1105-1113.
- [7] Barton, I. E. (1997). Laminar flow over a backward-facing step with a stream of hot particles. *International Journal of Heat and Fluid Flow*, 18(4), 400-410.
- [8] Inaoka, K., Nakamura, K., and Senda, M. (2004). Heat transfer control of a backward-facing step flow in a duct by means of miniature electromagnetic actuators. *International Journal of Heat and Fluid flow*, 25(5), 711-720.
- [9] Abu-Nada, E., Al-Sarkhi, A., Akash, B., and Al-Hinti, I. (2007). Heat transfer and fluid flow characteristics of separated flows encountered in a backward-facing step under the effect of suction and blowing. *Journal of Heat Transfer*, 129(11), 1517-1528.
- [10] Abu-Nada, E. (2008). Application of nanofluids for heat transfer enhancement of separated flows encountered in a backward facing step. *International Journal of Heat and Fluid Flow*, 29(1), 242-249.
- [11] Nie, J. H., Chen, Y. and Hsieh, H. T. (2009). Effects of a baffle on separated convection flow adjacent to backward-facing step. *International Journal of Thermal Sciences*, 48(3), 618-625.
- [12] Velazquez, A., Arias, J., and Mendez, B. (2008). Laminar heat transfer enhancement downstream of a backward facing step by using a pulsating flow. *International Journal of Heat and Mass Transfer*, 51(7), 2075-208
- [13] Suzuki, H., Kida, S., Nakamae, T., and Suzuki, K. (1991). Flow and heat transfer over a backward-facing step with a cylinder mounted near its top corner. *International Journal of Heat and Fluid flow*, 12(4), 353-359.
- [14] Tsay, Y. L., Chang, T. S., and Cheng, J. C. (2005). Heat transfer enhancement of backward-facing step flow in a channel by using baffle installation on the channel wall. *ActaMechanica*, 174(1-2), 63-76.
- [15] Cheng, J.-C. and Y.-L. Tsay (2006). Effects of solid and slotted baffles on the convection characteristics of backward-facing step flow in a channel. *Heat and mass transfer*, 42(9), 843-852.
- [16] Selimefendigil, F. and Öztop, H. F. (2013b). Numerical analysis of laminar pulsating flow at a backward facing step with an upper wall mounted adiabatic thin fin. *Computers & Fluids*, 88, 93-107.
- [17] Kumar, A. and Dhiman A. K. (2012). Effect of a circular cylinder on separated forced convection at a backward-facing step. *International Journal of Thermal Sciences*, 52, 176-185.
- [18] Selimefendigil, F. and Öztop, H. F. (2013a). Identification of forced convection in pulsating flow at a backward facing step with a stationary cylinder subjected to nanofluid. *International Communications in Heat and Mass Transfer*, 45, 111-121.
- [19] Selimefendigil, F. and Öztop, H. F. (2014). Control of Laminar Pulsating Flow and Heat Transfer in Backward-Facing Step by Using a Square Obstacle. *J. Heat Transfer* 136(8), 081701 (11 pages); Paper No: HT-12-1549; doi:10.1115/1.4027344
- [20] Chatterjee, D., Sengupta, A., Debnath, N and De, S (2015). Influence of an adiabatic square cylinder on hydrodynamic and thermal characteristics in a two-dimensional backward-facing step channel. *Heat Transfer Research*, 46(1), 63-89(2015).
- [21] Sekarapandian, N., Sanyasiraju, Y.V.S.S. and Vengadesan, S. (2009). A novel semi-explicit spatially fourth order accurate projection method for unsteady incompressible viscous flows. *Numerical Heat Transfer, Part A: Applications*, 56(8), 665-684.
- [22] Sekarapandian, N. (2014). Development of a novel compact finite difference scheme for incompressible flows. Ph.D thesis (Submitted), IIT Madras, India.
- [23] Brown, D. L., Cortez, R., and Minion, M. L. (2001). Accurate projection methods for the incompressible Navier-Stokes equations. *Journal of Computational Physics*, 168(2), 464-499.